Band anticrossing in highly mismatched semiconductor alloys

W Walukiewicz

Materials Sciences Division, Lawrence Berkeley National Laboratory, Berkeley, CA 94720

Abstract. The basic theoretical aspects of the band anticrossing effects in highly electronegativity-mismatched semiconductor alloys are reviewed. The many-impurity Anderson model treated in the coherent potential approximation is applied to the semiconductor alloys, in which metallic anion atoms are partially substituted by atoms of a highly electronegative element. Analytical solutions for the Green's function describe dispersion relations and state broadening effects for the restructured conduction band. The solutions are identical to those obtained from the physically intuitive and widely used two-level band anticrossing model. It is shown that the model explains key experimental observations including the unusual composition and pressure dependence of the interband optical transitions and the large enhancement of the electron effective mass.

1. Introduction

Alloying of semiconductor materials is frequently used to tailor the material properties for specific applications. Therefore, a significant effort has been devoted to understand the electronic structure of random semiconductor alloys. In a simplest approach based on the Virtual Crystal Approximation (VCA), the electronic properties of the alloys are given by the linear interpolation between the properties of the end-point materials [1,2]. The alloy disorder effects are typically included through a bowing parameter that describes the deviations from the VCA. Most of the studies of semiconductor alloy systems are restricted to the cases where there are only small differences between properties of the end-point semiconductors. Such "well-matched" alloys can be easily synthesized and their properties are close to the VCA predictions.

Recent progress in the epitaxial growth techniques has led to the successful synthesis of semiconductor alloys composed of materials with distinctly different properties. Thus, it has been shown that alloying of standard III-V compounds with group III-nitrides results in formation of new class of materials whose properties strongly depend on the alloy composition. For example, it has been found that incorporation of only 1% of N into GaAs to form $GaAs_{0.99}N_{0.01}$ reduces the energy gap by about 180 meV [3]. Similarly large band gap reductions were observed also in other group III-V_{1-x}-N_x alloys [4-7]. It has been shown recently that group III-V_{1-x}-N_x alloys belong to a much broader class of highly mismatched alloys (HMAs). Such alloys are formed when electronegative

(metallic) atoms substitute metallic (electronegative) atoms. An extreme case of HMAs is represented by group II-VI_{1-x}-O_x, where highly electronegative O partially replaces more metallic column VI anions [8].

The first attempts to explain the large effects observed in HMAs were based on a dielectric model that predicted highly nonlinear composition dependencies of the band gap for the alloys of semiconductor compounds with very different properties [9]. The model predicted a semiconductor to semi-metal transition in some of the alloys [9,10]. Later, several other theoretical explanations of the large band gap reduction in III-V-N alloys have been also proposed [11-16]. An extensive review of theoretical, experimental and applied aspects of group III-V-N alloys can be found in a series of recently published articles [17].

One of the salient features of the HMAs is that a replacement of the anion atoms with isoelectronic atoms with very much different electronegativity results in formation of localized electronic states. In the cases of substitution of N atoms in III-V compounds [18] or O atoms in II-VI compounds [19], the energy levels of the localized states are located close to the conduction band edge. At low, impurity-like concentrations, the impurity atoms give rise to complex photoluminescence spectra associated with excitons bound to isolated impurities and/or impurity pairs. At higher alloy-like impurity concentrations, the impurity states loose their localized character and form band through an interaction with extended states of the host semiconductor matrix. The alloying effects in HMAs have been described in terms of the two-level Band Anticrossing (BAC) model. This model has been developed to explain the pressure and composition dependencies of the band gap of $In_yGa_{1-y}As_{1-x}N_x$ alloys [20]. Later, it was successfully applied to other HMAs [8,21,22]. The BAC model has predicted several new effects, such as a N-induced enhancement of the electron effective mass [23], an improvement in the donor activation efficiency [24] in $In_yGa_{1-y}As_{1-x}N_x$ alloys, and the change in the nature of the fundamental band gap from indirect to direct in $GaP_{1-x}N_x$ [22]. All these predictions have been experimentally confirmed in recent experiments.

In this paper, we will review main results of the BAC model formulated within a coherent potential approximation (CPA). We will apply the model to different HMAs and discuss some of the consequences of the modified conduction band structure on the properties of different alloys.

2. Band Anticrossing model

In the BAC model, the restructuring of the conduction band is a result of an anticrossing interaction between highly localized A_1 states of substitutional highly electronegative atoms and the extended states of the host semiconductor matrix. The newly formed subbands, named E_+ and E_-, have dispersion relations given by [20]

$$E_{\pm}(k) = \frac{1}{2}\left\{ \left[E^C(k) + E^L\right] \pm \sqrt{\left[E^C(k) - E^L\right]^2 + 4V^2 \cdot x}\right\}, \quad (1)$$

where $E^C(k)$ is the energy dispersion of the lowest conduction band of the host, and E^L is the energy of the localized states derived from the substitutional N atoms. The coupling between the localized states and the band states of the host is described by the hybridization parameter V. The BAC model provides a simple, analytical expression to calculate the electronic and optical properties of III-V_{1-x}-N_x alloys.

The two-level BAC model is a result of degenerate perturbation theory applied to a system of localized states and extended states. The interaction between these two types of states has been treated in the simplest possible manner that does not account for expected severe level broadening effects. To account for these effects, we have used so called

many-impurity Anderson model that has been developed to describe the electronic properties of semiconductor crystals with low concentrations of transition-metal impurities [25-27]. Very recently, the many-impurity Anderson model has also been used to evaluate the interaction between the randomly distributed localized states and the extended states in HMAs [28].

In applying the Anderson model to HMAs, one considers an interaction between the localized states $|L\rangle$ and extended states $|\mathbf{k}\rangle$. For randomly spatially distributed impurities the configurational averaging can be carried out neglecting correlations between positions of the impurities. The Coherent Potential Approximation (CPA) is usually used to treat such systems [26]. In the CPA, consecutive multiple scatterings from each single impurity atom are fully taken into account, but correlations between scatterings from different impurity atoms are neglected due to the lack of coherence between the randomly distributed impurity sites. After the configurational averaging in the framework of CPA, the average Green's function restores the space translational invariance, and **k** resumes its well-defined properties as a good quantum number. In momentum space, the diagonal Green's function can be written as [26]

$$G_{\mathbf{kk}}(E)=\left[E-E_{\mathbf{k}}^{C}-\frac{V^{2}x}{E-E^{L}-i\boldsymbol{p}\boldsymbol{b}V^{2}\boldsymbol{r}_{0}(E^{L})}\right]^{-1}, \tag{2}$$

where V is the average hybridization parameter and $\boldsymbol{r}_0$ is the unperturbed density of states of $E_{\mathbf{k}}^{C}$ per unit cell. Since $\boldsymbol{r}_0$ only weakly depends on energy, it can be assumed to be a constant in the lowest order approximation, with an effective value equal to the unperturbed density of states evaluated at E^L and multiplied by a prefactor $\boldsymbol{b}$. The new dispersion relations are determined by the poles of $G_{\mathbf{kk}}(E)$, and the solutions are given by an equivalent two-level-like eigen-value problem,

$$\begin{vmatrix} E_{\mathbf{k}}^{C}-E(\mathbf{k}) & V\sqrt{x} \\ V\sqrt{x} & E^{L}+i\Gamma_{L}-E(\mathbf{k}) \end{vmatrix}=0, \tag{3}$$

where $\Gamma_L=\boldsymbol{p}\boldsymbol{b}V^{2}\boldsymbol{r}_{0}(E^{L})$ is the broadening of E^L in the original single-impurity Anderson Model [25].

If Γ_L=0, Eq.(3) is reduced to the two-level BAC model of Eq.(1) with two restructured dispersions for the upper and lower conduction subbands. The flattened and downshifted lower subband is responsible for most of the unusual effects, such as the drastic bandgap reduction and the electron effective mass enhancement. When the broadening Γ_L is nonzero but small, so that $2V\sqrt{x}>>\boldsymbol{p}\boldsymbol{b}V^{2}\boldsymbol{r}_{0}(E^{L})$ and $\left|E_{\mathbf{k}}^{c}-E^{L}\right|>>\boldsymbol{p}\boldsymbol{b}V^{2}\boldsymbol{r}_{0}(E^{L})$, one obtains an approximate analytical solution for Eq.(3),

$$\tilde{E}_{\pm}(\boldsymbol{k})\approx E_{\pm}(\boldsymbol{k})+i\Gamma_{L}\frac{\left[E_{\pm}(\boldsymbol{k})-E_{\boldsymbol{k}}^{C}\right]}{\left[E_{\pm}(\boldsymbol{k})-E_{\boldsymbol{k}}^{C}\right]+\left[E_{\pm}(\boldsymbol{k})-E^{L}\right]}\equiv E_{\pm}(\boldsymbol{k})+i\Gamma_{\pm}(\boldsymbol{k}), \tag{4}$$

where $E_{\pm}(\boldsymbol{k})$ is the real part of $\tilde{E}_{\pm}(\mathbf{k})$ and is defined in Eq.(1). The imaginary part of the dispersion relations defines the hybridization-induced energy uncertainties. It is worth noting that the imaginary part in Eq.(4) is proportional to the admixture of the localized states to the restructured wavefunctions in the two-level-perturbation picture described by Eq.(3),

$$\Gamma_{\pm}(\mathbf{k})=\left|\langle L\,|\,E_{\pm}(\mathbf{k})\rangle\right|^{2}\cdot\Gamma_{L}. \tag{5}$$

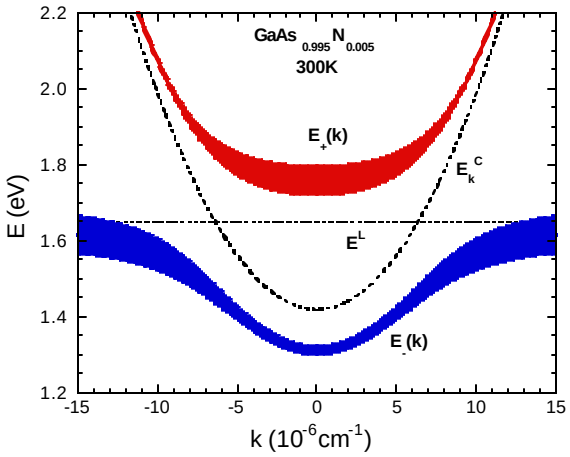

Figure 1. Calculated restructuring of the conduction band of $GaAs_{0.995}N_{0.005}$ alloys. The shaded area represents the magnitude of the level broadening.

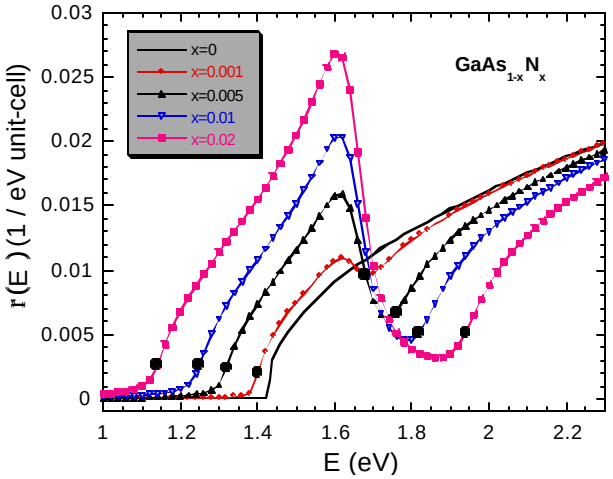

Figure 2. Density of states of $GaAs_{1-x}N_x$ alloys for few different compositions, x. The two dots on each curve represent the energies of the E_ and E+ subband edges.

As an example, Fig.1 shows the calculated dispersion relations for the subba nds given by Eq.(1) for $GaAs_{0.985}N_{0.015}$ near the Brillouin zone center. The broadenings of the dispersion relations are given by the imaginary part of Eq.(4).

It is interesting to see the effects of band anticrossing on the density of states of the conduction band. The density of states per unit cell for the unperturbed conduction band edge of GaAs is given by,

$$r_0(e) = 4p\sqrt{e - E_0^C}\,/\,e_B^{3/2}, \tag{6}$$

where $e_B = \hbar^2(2p/b)^2/(2m^*_{GaAs})$ is of the order of the conduction band width. b=5.65 Å is the lattice constant of the unit cell, and m^*_{GaAs} is the electron effective mass of GaAs.

The perturbed density of states can be calculated from the imaginary part of the Green's function and is given by the expression,

$$r(E)=\frac{1}{p}\,\mathrm{Im}\sum_{\mathbf{k}}G_{\mathbf{kk}}(E)=\frac{1}{p}\int r_0\left(E_{\mathbf{k}}^{C}\right)\mathrm{Im}[G_{\mathbf{kk}}(E)]\,dE_{\mathbf{k}}^{C}. \qquad (7)$$

The integration converges rapidly with $E_{\mathbf{k}}^{C}$ in a small range that is proportional to x. The calculated perturbed density of states for $GaAs_{1-x}N_x$ with several small values of x is shown in Fig. 2. It is seen in Figs. 1 and 2 that incorporation of N results in a drastic restructuring of the conduction band dispersion. It splits conduction band into two highly non-parablic subbands. We will show that this massive modification of the electronic structure leads to new, unusual phenomena in HMA's.

3. Comparison with experiment

3.1. Fundamental energy gap

The bandgap reduction in $GaAs_{1-x}N_x$ alloys results from the downward shift of the conduction band edge E_(k=0) caused by the anticrossing interaction. Figure 3 shows experimental values of the fundamental bandgap as a function of N concentration from various reports [3, 29-31] together with the dependence calculated from Eq. (1). The best fit to experimental data is obtained assuming the interaction constant V=2.7eV. It is important to note that the composition dependence cannot be explained by a constant, composition independent bowing parameter. Most recent attempt to explain this dependence in terms of a phenomenological composition dependent bowing function required five fitting parameters [32].

As seen in Figs. 1 and 2, an important feature of the restructured conduction band is the existence of two subbands with minima at E_(k=0) and E+(k=0). These minima give rise to two well resolved absorption edges that were observed in photo- and electro-modulated reflection [20,33] as well as in direct absorption measurements [34]. Key experiments that led to the formulation of the BAC model were hydrostatic pressure measurements of the photomodulated reflection (PR) [20]. Figure 4 shows pressure dependence of the optical transitions to E_ and E+ edges. Since E^{L} and $E^{C}(k=0)$ have very much different pressure coefficients one can clearly observe characteristic pressure induced anticrossing behavior. It is also worth noting the pressure induced change in the nature of the subband edges from mostly extended (localized) for E_ (E+) at the ambient pressure to mostly localized (extended) at high pressures.

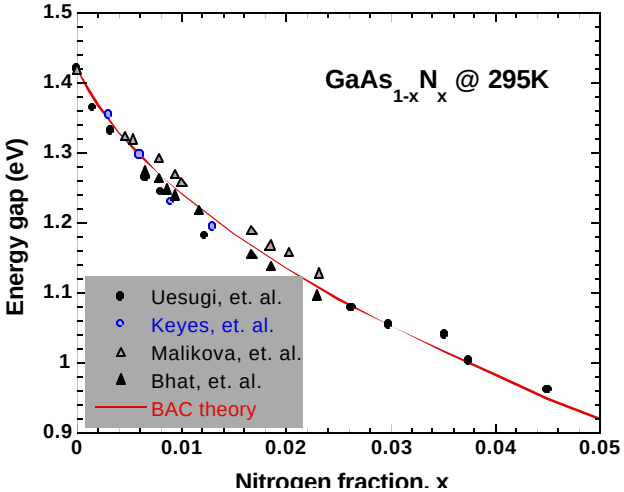

Figure 3. Energy gap vs. N content from Refs. [3, 29-31]. The solid curve represents the BAC model based calculations.

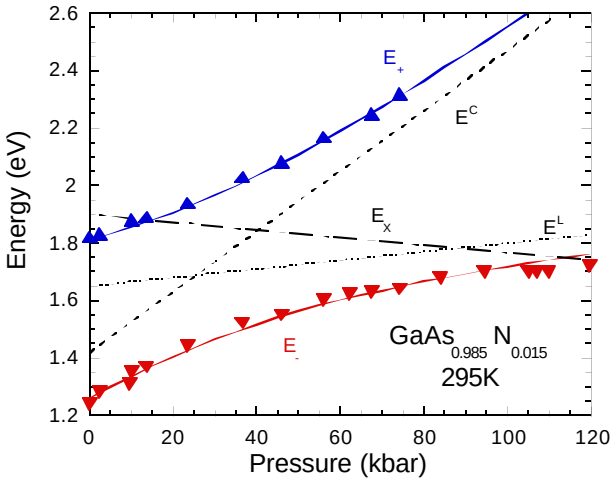

Figure 4. Hydrostatic pressure dependence of the E_ and E+ subband edges.

Although InGaNAs has been the most extensively studied alloy system, similar band anticrossing effects have also been observed in several other N-containing III-V alloys, such as $GaP_{1-x}N_x$ [4], $InP_{1-x}N_x$ [5], $GaSb_yAs_{1-x-y}N_x$ [6] and $InSb_{1-x}N_x$ [7].

3.2. Electron effective mass

As is seen in Fig. 1, the anticrossing interaction between the localized N-states and the conduction band leads to a drastic modification of the conduction band dispersion. From the predicted flattening of the dispersion curve for the lowest conduction band E_(k), one expects a large N-induced changes in the value and energy dependence of the electron effective mass. Indeed, a series of recent experiments have confirmed these predictions. Large enhancements of the electron effective mass were deduced from measurements of the plasma reflection edge [23,35] and optically detected magnetic resonance [36] in InGaNAs and from interband optical transitions in GaNAs/GaAs quantum wells [37].

Especially compelling evidence in support of the BAC model has been provided by measurements of the plasma reflection on a series of $In_{0.03}Ga_{0.97}As_{0.99}N_{0.01}$ samples with

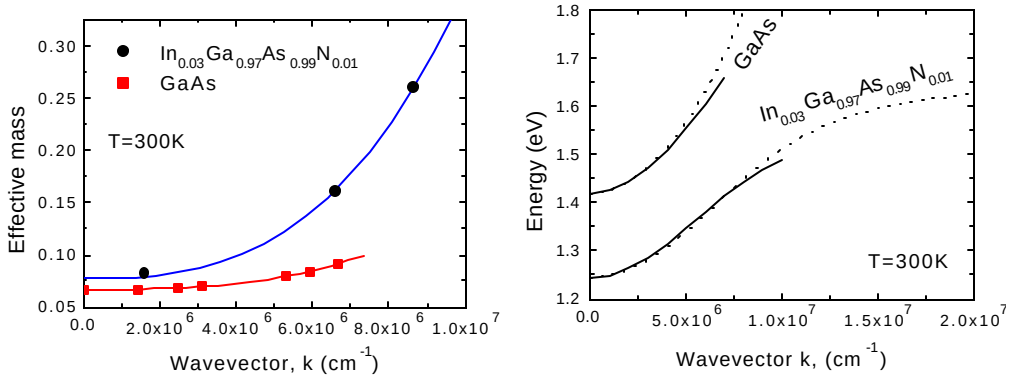

(a) (b)

Figure 5. (a) The electron effective mass vs. Fermi wavector in $In_{0.97}Ga_{0.03}As_{0.99}N_{0.01}$ and in GaAs. (b) Dispersion relation E(k) for the lowest conduction band calculated from the experimental results shown in Fig. 5 (a).

varying electron concentration [35]. As shown in Fig. 5 (a), the effective mass is rapidly increasing with increasing electron wavevector, k that is determined by the electron concentration, n through the relation, $k=(3\pi^2 n)^{1/3}$. Results for the k-vector dependence of the effective mass in GaAs are also shown for comparison. Using the standard definition of the effective mass m* and the experimental m*(k) dependence, one can determine the dispersion relation E(k) for the lowest conduction subband [35]. The results are shown in Fig. 5 (b). It is seen that the experimentally determined E(k) dependence for the $In_{0.03}Ga_{0.97}As_{0.99}N_{0.01}$ alloys (solid line) is in a very good agreement with dispersion relation for E_(k) subband calculated from the BAC model (dashed line). It should be emphasized that since the previously determined value of V=2.7 eV is used for the hybridization parameter, there are no adjustable parameters in these calculations.

4. Conclusions

Since their discovery more than 10 years ago, GaInNAs alloys were very extensively studied by many research groups. At the beginning the interest was generated mostly by potential applications of these materials for optoelectronic devices [17]. However, it has been recognized very early that understanding of the unusual properties of these materials will require reexamination of the existing theories of the electronic structure of semiconductor alloys. It has been also shown that the III-V-N alloys are only a subset of a much broader class of highly mismatched alloys whose properties are determined by the electronegativity mismatch of the constituent elements. The theoretical approach developed to understand properties of III-V-Ns has been successfully applied to HMAs ranging from very highly mismatched II-VI_{1-x}-O_x to moderately mismatched $GaSb_{1-x}As_x$ $GaSb_{1-x}P_x$ alloys [38].

This work was supported by the Director, Office of Science, Office of Basic Energy Sciences, Division of Materials Sciences and Engineering, of the U.S. Department of Energy under Contract No. DE-AC03-76SF00098.

References

[1] Van Vechten J A and Bergstresser T K 1970 Phys. Rev. B 1 3351
[2] Hill R and Richardson D 1971 J. Phys. C 4 L289
[3] Weyers M, Sato M, and Ando H 1992 Jpn. J. Appl. Phys. 31 L853; Uesugi K, Marooka N, and Suemune I 1999 Appl. Phys. Lett. 74 1254
[4] Baillargeon N, Cheng K Y, Hofler G F, Pearah P J, and Hsieh K. C. 1992 Appl. Phys. Lett. 60 2540
[5] Bi W G and Tu C W 1996 Appl. Phys. Lett. 80 1934
[6] Harmand J C, Ungaro G, Ramos J, Rao E V K, Saint-Girons G, Teissier R, Le Roux G, Largeau L, and Patriarche G 2000 J. Cryst. Growth 227-228 553
[7] Murdin B N, Karmal-Saadi M, Lindsay A, O'Reilly E P, Adams A R, Nott G J, Crowder J G, Pidgeon C R, Bradley I V, Wells J P R, Burke T, Johnson A D, and Ashley T 2001 Appl. Phys. Lett. 78 1558
[8] Yu K M, Walukiewicz W, Wu J, Beeman J W, Ager J W III, Haller E E, Miotkowski I, Ramdas A K, and Becla P 2002 Appl. Phys. Lett. 80 1571
[9] Van Vechten J A 1969 Phys. Rev. 187 1007 (1969)
[10] Sakai S, Ueta Y, and Terauchi Y 1993 Jpn. J. Appl. Phys. Part 1 32 4413
[11] Neugebauer J, Van de Walle C G 1995 Phys. Rev. B 58 10658
[12] Jones E D, Modine N A, Allerman A A, Kurtz S R, Wright A F, Tozer S T, and Wei X 1999 Phys. Rev. B 60 4430

[13] Mattila T, Wei S -H, and Zunger A 1999 Phys. Rev. B 60 R11245

[14] Wang L -W 2001 Appl. Phys. Lett. 78 1565; Szwacki N G and Boguslawski P 2001 Phys. Rev. B 64 161201

[15] Al-Yacoub A and Bellaiche L 2000 Phys. Rev. B 62 10847

[16] Zhang Y, Mascarenhas A, Xin H P, and Tu C W 2001 Phys. Rev. B 63 161303

[17] see special issue of Semicond. Sci. Technol. 2002 Vol. 17 No. 8

[18] Hjalmarson, H P, Vogl P, Wolford D J, and Dow J D 1980 Phys. Rev. Lett. 44 810

[19] Seong M J, Alawadhi H, Miotkowski I, Ramdas A K and Miotkowska S 2000 Phys. Rev. B 62 1866

[20] Shan W, Walukiewicz W, Ager J W III, Haller E E, Geisz J F, Friedman D J, Olson J M, and Kurtz S R 1999 Phys. Rev. Lett. 82 1221

[21] Walukiewicz W, Shan W, Yu K M, Ager J W III, Haller E E, Miotkowski I, Seong M J, Alawadhi H and Ramdas A K 2000 Phys. Rev. Lett. 85 1552

[22] Shan W, Walukiewicz W, Yu K M, Wu J, Ager J W III, Haller E E, Xin H P, and Tu C W 2000 Appl. Phys. Lett. 76 3251

[23] Skierbiszewski C, Perlin P, Wisniewski E, Knap W, Suski T, Walukiewicz W, Shan W, Yu K M, Ager J W III, Haller E E, Geisz J F, and Olson J M 2002 Appl. Phys. Lett. 76 2409

[24] Yu K M, Walukiewicz W, Shan W, Ager J W III, Wu J, Haller E E, Geisz J F, Friedman D J, and Olson J M 2000 Phys. Rev. B 61 R13337

[25] Anderson P W Phys. Rev. 1961 124 41

[26] Kocharyan A N, Soc. Phys. 1986 Solid State 28 6

[27] Ivanov M A and Pogorelov Yu G 1979 Sov. Phys. JETP 49 510; Ivanov M A and Pogorelov Yu G 1985 Sov. Phys. JETP 61 1033

[28] Wu J, Walukiewicz W, and Haller E E 2002 Phys. Rev. B 65 233210

[29] Keyes B M, Geisz J F, Dippo P C, Reedy R, Kramer C, Friedman D J, Kurtz S R, and Olson J M 1999 NCPV Photovoltaics Program Review, AIP Conference Proceedings 462 511

[30] Malikova L, Pollak F H and Bhat R J 1998 Electron. Mat. 27 484

[31] Bhat R, Caneau C, Salamanca-Riba L, Bi W, and Tu C 1998 J. Cryst. Growth 195 427

[32] Tisch U, Finkman E, and Salzman J 2002 Appl. Phys Lett. 81 463

[33] Perkins J D, Mascarenhas A, Zhang Y, Geisz J F, Friedman D J, Olson J M, and Kurtz S R 1999 Phys. Rev. Lett. 82 3312

[34] Perlin P, Wisniewski P, Skierbiszewski C, Suski T, Kaminska E, Subramanya S G, Weber E R, Mars D E, and Walukiewicz W 2000 Appl. Phys. Lett. 76 1279 (2000).

[35] Skierbiszewski C, Perlin P, Wisniewski P, Suski T, Geisz J F, Hingerl K, Jantsch W, Mars D E, and Walukiewicz W 2002 Phys. Rev. B 65 035207

[36] Hai P N, Chen W M, Buyanova I A, Xin H P, and Tu C W 2000 Appl. Phys. Lett. 77 1843

[37] Wu J, Shan W, Walukiewicz W, Yu K M, Ager J W III, Haller E E, Xin H P, and Tu C W 2001 Phys. Rev. B 64 85320

[38] Wu J, Shan W, and Walukiewicz W 2002 Semicond. Sci. Technol. 17 860